

See discussions, stats, and author profiles for this publication at: <https://www.researchgate.net/publication/26705357>

# Self-Assembled Cylindrical and Vesicular Molecular Templates for Polyaniline Nanofibers and Nanotapes

ARTICLE *in* THE JOURNAL OF PHYSICAL CHEMISTRY B · AUGUST 2009

Impact Factor: 3.3 · DOI: 10.1021/jp9043418 · Source: PubMed

---

CITATIONS

35

READS

21

## 2 AUTHORS:



Anilkumar Parambath

University of British Columbia - Vancouver

28 PUBLICATIONS 792 CITATIONS

[SEE PROFILE](#)



Manickam Jayakannan

Indian Institute of Science Education and ...

74 PUBLICATIONS 1,566 CITATIONS

[SEE PROFILE](#)

## Self-Assembled Cylindrical and Vesicular Molecular Templates for Polyaniline Nanofibers and Nanotapes

P. Anilkumar<sup>†</sup> and M. Jayakannan<sup>\*,‡</sup>

*Chemical Sciences and Technology Division, National Institute for Interdisciplinary Science and Technology, Thiruvananthapuram-695019, Kerala, India, and Department of Chemistry, Indian Institute of Science Education and Research (IISER), NCL Innovation Park, Dr. Homi Bhabha Road, Pune 411008, India*

Received: May 10, 2009; Revised Manuscript Received: June 30, 2009

We report a soft template approach based on a custom-designed novel surfactant-cum-dopant for size and shape tuning of polyaniline nanomaterials such as nanofibers and nanotapes via emulsion and dispersion polymerization routes. A new amphiphilic 4-(3-dodecyl-8-enylphenyloxy) butane sulfonic acid was synthesized by ring-opening of butanesultone with renewable resource cardanol. The new amphiphilic dopant forms spherical micelles in water and its critical micelle concentration was determined by dye encapsulation and surface tension methods. In the emulsion route, the amphiphilic dopant complexed with aniline to produce cylindrical micellar aggregates that template exclusively for polyaniline nanofibers. The dispersion of aniline + dopant in water/toluene solvent mixture produces vesicles that selectively template for polyaniline nanotapes. The mechanism of the polyaniline nanomaterials formation was investigated by dynamic light scattering (DLS) and high-resolution transmission electron microscopy (HR-TEM). DLS of the polymerization templates in water proved the presence of micrometer range aggregates, and TEM images confirmed the shape of the cylindrical and vesicular templates. The polyaniline nanomaterials were found soluble in water and polar organic solvents for structural characterization and composition analysis by <sup>1</sup>H NMR spectroscopy. Absorbance spectra of the nanomaterials showed free carrier tail above 900 nm in the near IR region for the delocalization of electrons in the polaron band corresponding to expanded conformation of polyaniline chains. Wide angle X-ray diffraction showed two new peaks at low angle region with *d*-spacing of 26.5 and 13.6 Å corresponding to lamellar ordering of polyaniline chains followed by interdigitations of the amphiphilic dopant in the nanomaterials.

### Introduction

Polyaniline nanomaterials have attained wide interest due to their unique electrochemical properties and processability<sup>1–3</sup> in electronic and optical devices such as energy storage devices,<sup>4</sup> electron field emitters,<sup>5</sup> chemical sensors,<sup>6,7</sup> biological sensors,<sup>8,9</sup> actuators,<sup>10</sup> and so forth. Polyaniline one-dimensional nanostructures were synthesized using hard templates like alumina and zeolites,<sup>11</sup> soft templates like gels, and liquid crystal,<sup>13</sup> emulsion,<sup>14,15</sup> dispersion,<sup>16,17</sup> interfacial<sup>18</sup> seeding<sup>4</sup> and dilute polymerizations methods,<sup>19</sup> and so forth. Commercial available mineral acids or custom designed sulfonic acids such as camphor sulfonic acid, naphthalene sulfonic acid, p-toluene sulfonic acid, and azobenzene sulfonic acid were utilized as dopants for polyaniline nanomaterials.<sup>20–24</sup> Among all the approaches, emulsion and dispersion routes have been paid more importance due to the formation of high quality nanomaterials and the adaptability to simple synthetic conditions.<sup>2,25</sup> Most often, the synthesis of polyaniline nanomaterials via emulsion route were found highly susceptible to the dopant/aniline ratio in the feed, and uniform morphology of the nanomaterials were produced only for selected compositions.<sup>2,20</sup> In dispersion polymerization, the precipitation of the polyaniline is usually prevented by adding steric stabilizers such as cellulose derivatives that produce polyaniline composite nanomaterials rather

than pure polyaniline nanomaterials.<sup>16,17,26</sup> Self-stabilized dispersion method was also reported in which the anilinium ions act as interfacial stabilizer for the water–oil dispersion; however, poor control over the polyaniline morphology was observed.<sup>27</sup> The reason for the in-homogeneity in the morphology control in both these cases was correlated to poor and unstable micelles formation of aniline-dopant complex in water.<sup>2,20</sup> Further, polyaniline nanomaterial formation was found highly sensitive to experimental parameters such as ultrasonic stirring,<sup>28</sup> magnetic stirring,<sup>29</sup> rate of mixing,<sup>30</sup> reaction time<sup>31</sup> and temperature,<sup>32</sup> reactants compositions and concentrations,<sup>33</sup> and so forth. Additionally, there is a large discrepancy in the selection of dopant for specific polymerization routes, for example, an emulsion friendly dopant is not suitable candidate for dispersion route and vice versa.<sup>2,3</sup> Camphor sulfoic acid is a very good candidate for dispersion route and is not suitable for emulsion polymerization.<sup>34</sup> Similarly, dodecylbenzene sulfonic acids (DBSA) form stable micellar template for emulsion route but are not suitable for dispersion routes<sup>35</sup> (also for interfacial route). In our previous studies, we had attempted to address some of these issues by the way of designing a new amphiphilic molecule, 4-[4-hydroxy-2 ((Z)-pentadec-8-enyl) phenyl]-azobenzene sulfonic acid, and utilized it as a structure-directing agent for polyaniline nanomaterials (also for polypyrrole).<sup>36–41</sup> The morphologies of the conducting structures such as nanofibers, rods, tubes, and spheres were successfully tuned via emulsion, interfacial, and dilution polymerization routes. However, the amphiphilic azobenzene sulfonic acid dopant was found not

\* To whom correspondence should be addressed. E-mail: jayakannan@iiserpune.ac.in. Fax: 0091-20-25898022.

<sup>†</sup> National Institute for Interdisciplinary Science and Technology.

<sup>‡</sup> Indian Institute of Science Education and Research (IISER).

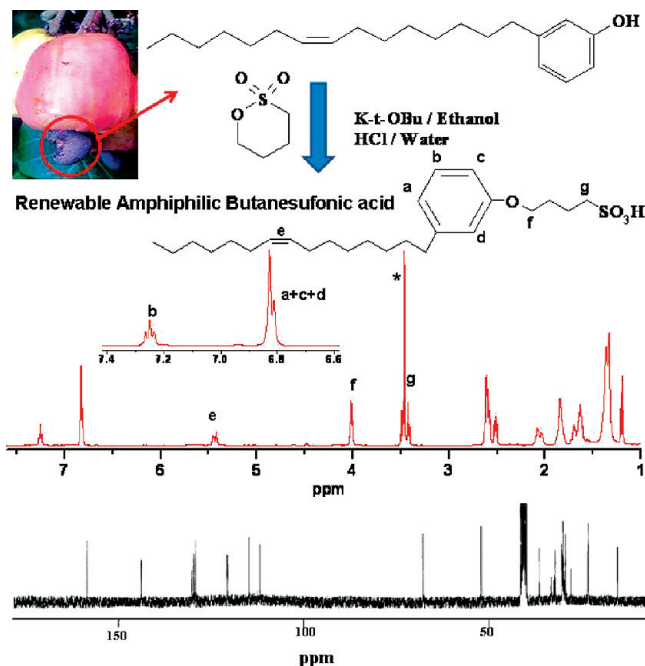


**Figure 1.** Schematic representation of the synthesis of dopant and its  $^1\text{H}$  and  $^{13}\text{C}$  NMR spectra in  $\text{d}_6\text{-DMSO}$ .

suitable for dispersion polymerization. Therefore, the development of single dopant-based templates for both emulsion and dispersion routes is still an unsolved problem in polyaniline nanostructures (also for other types of nanomaterials). We believe that it is an important issue to be addressed because of the following reasons: (i) single dopant-based approach for emulsion and dispersion routes is attractive since tuning of nanostructures can be done without altering the chemical constituents, (ii) understanding the mechanistic aspects of emulsion and dispersion routes is essential for fundamental nanomaterial research, (iii) study the effect of polymerization routes on the size and shape of the polyaniline nanomaterials, (iv) and finally among all the synthetic approaches known for nanomaterials, only emulsion and dispersion routes have the possibility for large scale production.

The present work emphasizes developing a novel amphiphilic surfactant-cum-dopant Z-4-(3-pentadec-8-enyl)phenoxy)-butane-1-sulfonic acid (see Figure 1) by ring-opening of 1,4-butanesultone with cardanol (3-pentadec-8-enyl-phenol, an industrial waste from cashew nut industry) under basic conditions. The newly designed dopant almost looks like commercial dodecyl benzene sulfonic acid (DBSA, available in propanol solution), but bears aliphatic sulfonic acid groups. Unlike DBSA, the new molecule is a crystalline solid, thermally stable, and easy to handle under atmospheric conditions. We continued our interest in developing new dopant based on renewable resources because we believe that conducting polymers or nanomaterials from natural resources are very attractive due to their wide availability and lower cost and provide new opportunities for fundamental and applied research. The newly synthesized amphiphilic sulfonic acid dopant was employed as a structural directing agent for producing novel nanostructures by emulsion and dispersion polymerization routes. The dopant has built-in head-to-tail molecular design for amphiphilic nature and forms stable emulsion with aniline in water in wider compositions. The amphiphilic molecule was found to exist as 5.3 nm micelles in water. The micelle behavior of the dopant and its critical micelle concentration (CMC) was studied by surface tension, dye-encapsulation, and dynamic light scattering measurements. The

dopant micelle was found to produce cylindrical self-organized templates with aniline in emulsion route and produced well-defined polyaniline nanofibers. In water/toluene solvent mixtures (in dispersion route), the dopant + aniline complex transformed into vesicles that exclusively yielded polyaniline nanotubes. The amphiphilic molecule solubilizes the resultant nanomaterials in water and other organic solvents that facilitate the complete structural characterization by  $^1\text{H}$  NMR, FT-IR, and viscosity techniques. The mechanism of the nanomaterials formation was further studied in detail by dynamic light scattering (DLS) and high-resolution transmission electron microscopy (HR-TEM). The nanomaterials were characterized by SEM, TEM, absorption spectroscopy, and wide-angle X-ray diffraction to understand the morphology, electronic, and solid-state ordering properties. X-ray analysis revealed that the resultant nanomaterials were highly crystalline and possessed lamellar-type self-organization in the solid state that contributes to their high electrical conductivity in the range of 1–10 S/cm.

## Experimental Procedures

**Materials.** Aniline, ammonium persulfate (APS), 1,4-butanesultone, potassium tertiary butoxide, and hydrochloric acid were purchased from Aldrich chemicals. Cardanol was purified by double vacuum distillation at 3–4 mm of Hg and the fraction distilled at 220–235 °C was collected.<sup>36,42</sup>

**General Procedures.** The NMR analysis of the samples was carried out in 500-MHz Bruker Avance ii NMR Spectrometer at 30 °C. The purity of the compounds was determined by JEOL JSM600 fast atom bombardment (FAB) mass spectrometry. For SEM measurements, polymer samples were subjected to thin gold coating using JEOL JFC-1200 fine coater. The probing side was inserted into JEOL JSM- 5600 LV scanning electron microscope for taking photographs. Transmission electron microscope images were recorded using a FEI Tecnai 30G<sup>2</sup> S Twin HRTEM instrument at 100 kV. For TEM measurements, the water suspension of nanomaterials were prepared under ultrasonic stirring and deposited on Formvar-coated copper grid. Wide-angle X-ray diffractions of the finely powdered polymer samples were recorded by Philips Analytical diffractometer using CuK-alpha emission. For DLS measurements, we have used a Nano ZS Malvern instrument employing a 4 mW He–Ne laser ( $\lambda = 632.8$  nm) and equipped with a thermostated sample chamber. For all the DLS measurements, HPLC quality (Merck, India) double distilled water is used. Infrared spectra of the polymers were recorded using a Perkin-Elmer, spectrum one FTIR spectrophotometer in the range of 4000 to 400  $\text{cm}^{-1}$ . For conductivity measurements, the polymer samples were pressed into a 10 mm diameter disk and analyzed using a Keithley four probe conductivity instrument. The resistivity of the samples was measured at five different positions and at least two pellets were measured for each sample; the average of 10 readings was used for conductivity calculations. Thermal analyses of the samples were performed with a PerkinElmer Pyris-6 differential scanning calorimetry (DSC) instrument under nitrogen at a heating rate of 5 °C/min, and the instrument was calibrated with indium, tin, and lead standards. The thermal stability of the polymers was determined using TGA-50 Shimadzu Thermo gravimetric Analyzer (TGA) at a heating rate of 10 °C/min in nitrogen. UV-vis spectra of the PANI in water were recorded using Perkin-Elmer Lambda-35 UV-vis Spectro Photometer. The cyclic voltammetry of the nanomaterials was done using a CHI 1121A model (CH Instruments) electrochemical analyzer. For electrochemical experiments, the samples in PANI-EB form, which are well dispersed in 1 M HCl solution, are used. Cyclic

**TABLE 1: Concentration and Amount of Dopant, Conductivity, Dimensions, and WXRD-Data of Polyaniline Nanomaterials**

sample <sup>a</sup>	dopant conc (M)	amount of dopant <sup>b</sup> (in mole %)	conductivity (S/cm) <sup>c</sup>	nanomaterial dimensions <sup>d</sup>	WXRD <i>d</i> -spacing (Å) <sup>e</sup>
<b>E-10</b>	$5.5 \times 10^{-2}$	0.42	$0.9 \times 10^{-1}$ (4.2)	F, $100 \pm 20$ nm	25.6, 13.8, 4.8, 3.5, 2.1
<b>E-50</b>	$1.1 \times 10^{-2}$	0.39	$1.3 \times 10^{-1}$ (1.3)	F, $100 \pm 50$ nm	26.5, 3.6, 2.1, 2.1
<b>E-75</b>	$7.3 \times 10^{-3}$	0.21	$4.4 \times 10^{-1}$ (2.2)	F, $100 \pm 35$ nm	26.7, 13.7, 4.6, 3.5, 1.8
<b>E-100</b>	$5.5 \times 10^{-3}$	0.21	$0.8 \times 10^{-1}$ (6.9)	F, $100 \pm 25$ nm	26.4, 4.6, 3.5, 2.1
<b>D-10</b>	$5.5 \times 10^{-2}$	0.28	$0.3 \times 10^{-1}$ (0.2)	T, $1 \pm 0.5$ μm	24.7, 13.7, 4.7, 3.5, 2.1
<b>D-50</b>	$1.1 \times 10^{-2}$	0.13	$0.5 \times 10^{-1}$ (0.7)	T, $175 \pm 50$ nm	25.4, 13.8, 4.7, 3.5, 2.1
<b>D-75</b>	$7.3 \times 10^{-3}$	0.14	$1.1 \times 10^{-1}$ (8.8)	T, $150 \pm 50$ nm	25.3, 13.8, 4.4, 3.5, 2.1
<b>D-100</b>	$5.5 \times 10^{-3}$	0.05	$3.2 \times 10^{-1}$ (7.1)	T, $200 \pm 50$ nm	26.2, 13.7, 4.8, 3.5, 2.1

<sup>a</sup> Concentration of aniline was fixed as 0.55 M and in the name of the samples **E-X** and **D-X**, where X = [aniline]/[dopant]. <sup>b</sup> Determined by <sup>1</sup>H NMR spectroscopy. <sup>c</sup> Determined by four probe conductivity unit at 30 °C. The values given in the parentheses is that of *m*-cresol cast film. <sup>d</sup> F-nanofibers and T-nanotapes. The average sizes were calculated from SEM images. <sup>e</sup> Wide-angle X-ray diffraction measurements were done for powdered sample at 30 °C.

voltammograms were recorded using a platinum electrode at a scan rate of 100 mV s<sup>-1</sup>, using Calomel reference electrode and a Pt wire counter electrode.

**Synthesis of (Z)-4-(3-Pentadec-8-enyl) phenoxy) butane-1-sulfonic Acid (Dopant).** Distilled cardanol (10 g, 33 mmol) was added into a round-bottom flask containing potassium tertiary butoxide (7.52 g, 66 mmol) in dry ethanol (100 mL). The solution was warmed for 30 min under nitrogen atmosphere. It was cooled, 1,4-butanesultone (9 g, 66 mmol) was added dropwise, and then the reaction mixture was refluxed for 40 h under nitrogen atmosphere. It was cooled and the precipitate was isolated by filtration. The solid mass was dissolved in water (30 mL) and acidified by HCl solution (30 mL of 50% v/v HCl). The white mass was further purified by passing through silica gel column using 20/80 v/v methanol/chloroform as eluent. Yield = 6.5 g (45%). mp = 56–62 °C. <sup>1</sup>H NMR (DMSO-d<sub>6</sub>, 500 MHz) δ: 7.26 (t, 1H, Ar–H), 6.83 (b, 3H, Ar–H), 5.44 (b, 2H, –CH=CH–), 4.02 (t, 2H, Ar-OCH<sub>2</sub>), 3.42 (t, 2H, HO<sub>3</sub>SCH<sub>2</sub>), 3–0.8 (27H, aliphatic). <sup>13</sup>C NMR (DMSO-d<sub>6</sub>, 125 MHz) δ: 158.1, 143.8, 130.1, 129.6, 129.1, 120.3, 114.3, 111.4, 67.1, 51.1, 35.2, 30.8, 28.9, 28.6, 28.5, 26.5, and 13.9. FT-IR (KBr, cm<sup>-1</sup>): 3450.5, 2926.3, 2852.8, 1646.4, 1583.4, 1452.7, 1384.2, 1264.1, 1174.2, 1054.2, 970.1, 876.1, 786.3, 734.1, 692.3, 613.8, and 529.8. FAB-MS (MW, 438.0): *m/z* = 461.1 (M + Na).

**Dispersion Route for Polyaniline Nanomaterials.** The synthesis of polyaniline is described in detail for **D-100** and other samples were prepared following the same procedure. The dopant (0.048 g, 0.11 mmol) was dissolved in doubly distilled water (20 mL) in a 50 mL glass vial. In a separate glass vial, distilled aniline (1 mL, 1.02 g, 11 mmol, [aniline]/[dopant] = 100) was dissolved in toluene. To the dopant solution, aniline in toluene was added and the mixture was sonicated for 1 h to obtain a milky white dispersion. Ammoniumpersulfate solution (1.35 M) was added to the dispersion and stirred under ultrasonic for 5 min at 30 °C. The polymerization was allowed to continue at 30 °C for 15 h without further disturbance. The dark green polyaniline solid mass was filtered, washed with distilled water and methanol several times until the filtrate become colorless. The solid product was dried in a vacuum oven at 60 °C for 48 h (0.01 mmHg). Yield = 0.67 g (65%). <sup>1</sup>H NMR (DMSO-d<sub>6</sub>, 500 MHz) δ: 0.5–4.5 (aliphatic-H, dopant) 5.43 (b, CH=CH, dopant), 5.91(–N–H, PANI), 6.83 (b, Ar–H, dopant), 7.11, 7.21, 7.31 (1/1/1 triplet, –NH<sup>+</sup>, PANI), 7.25 (b, Ar–H, dopant), 7.35 (t, Ar–H, PANI), 7.48 (d, Ar–H, PANI), 7.55 (t, Ar–H, PANI). FT-IR (KBr, in cm<sup>-1</sup>): 3011.1, 1577.7, 1502.1, 1306.1, 1225.1, 1158.9, 1032.2, 825, 706, and 627.7.

**Emulsion Route for Polyaniline Nanomaterials.** Typical procedure for the synthesis of polyaniline nanofiber is described

in detail for **E-100** and other samples were prepared following the same procedure. The dopant (0.048 g, 0.11 mmol) was dissolved in doubly distilled water (20 mL) in a 50 mL glass vial. Distilled aniline (1 mL, 1.02 g, 11 mmol, [aniline]/[dopant] = 100) was added to the dopant solution in water and stirred under ultrasonic for an additional 1 h at 30 °C. At the end of the stirring, the formation of milky white emulsion was noticed. Ammonium persulfate (1.35 M solution) was added at 30 °C and stirred under ultrasonic for 1 more hour. The resultant green content was allowed to polymerize at 30 °C for 15 h without disturbance. The solid mass was filtered then washed with distilled water and methanol several times until the filtrate became colorless. The solid product was dried in a vacuum oven at 60 °C for 48 h (0.01 mmHg). Yield = 0.78 g (76%). <sup>1</sup>H NMR (DMSO-d<sub>6</sub>, 500 MHz) δ: 0.5–4.5 (aliphatic-H, dopant) 5.43 (b, CH=CH, dopant), 5.91(–N–H, PANI), 6.83 (b, Ar–H, dopant), 7.11, 7.21, 7.31 (1/1/1 triplet, –NH<sup>+</sup>, PANI), 7.25 (b, Ar–H, dopant), 7.35 (t, Ar–H, PANI), 7.48 (d, Ar–H, PANI), 7.55 (t, Ar–H, PANI). FT-IR (in cm<sup>-1</sup>): 3010.8, 1579.7, 1500.6, 1305.8, 1224.8, 1159.2, 1031.9, 825, 705.9 and 628.7.

The polyaniline nanomaterials **D-10**, **D-50**, **D-75**, **E-10**, **E-50**, and **E-75** were prepared by varying [aniline]/[dopant] ratio as 10, 50, and 75 (in moles) by following the above dispersion and emulsion procedures. The compositions and concentration of dopant are summarized in Table 1.

## Results and Discussion

A new renewable resource amphiphilic butane sulfonic acid was synthesized by reacting cardanol with 1,4-butanesultone using KtOBu as a base. The synthesis of the dopant is given in Figure 1. The structure of the dopant was confirmed by <sup>1</sup>H NMR, <sup>13</sup>C NMR, FT-IR, and Mass techniques (see Supporting Information). NMR spectrum of the dopant is shown in Figure 1, and the different types of the protons were assigned by alphabets. The four protons in the aromatic ring appear with characteristic splitting pattern at 7.26 and 6.83 ppm. The double bond in the pendent alkyl chain appears at 5.44 ppm, and the protons with respect to Ar-OCH<sub>2</sub> and CH<sub>2</sub>-SO<sub>3</sub>H appeared at 4.02 and 3.42, respectively. All other aliphatic protons appear below 3 ppm. The <sup>13</sup>C NMR spectrum also showed 8 peaks above 100 ppm corresponding to 6 aromatic and 2 vinylene carbon atoms. The peak intensities are in accordance to the expected structure, which confirms the formation of the new renewable resource amphiphilic dopant. FT-IR analysis (see Supporting Information) showed a broad peak at 3454 cm<sup>-1</sup> that corresponds to the –OH stretching of the sulfonic acid group.<sup>36</sup> The peak at 1610 and 1456 cm<sup>-1</sup> were assigned to C=C vibrations of olefin and aromatic rings, respectively. The peak

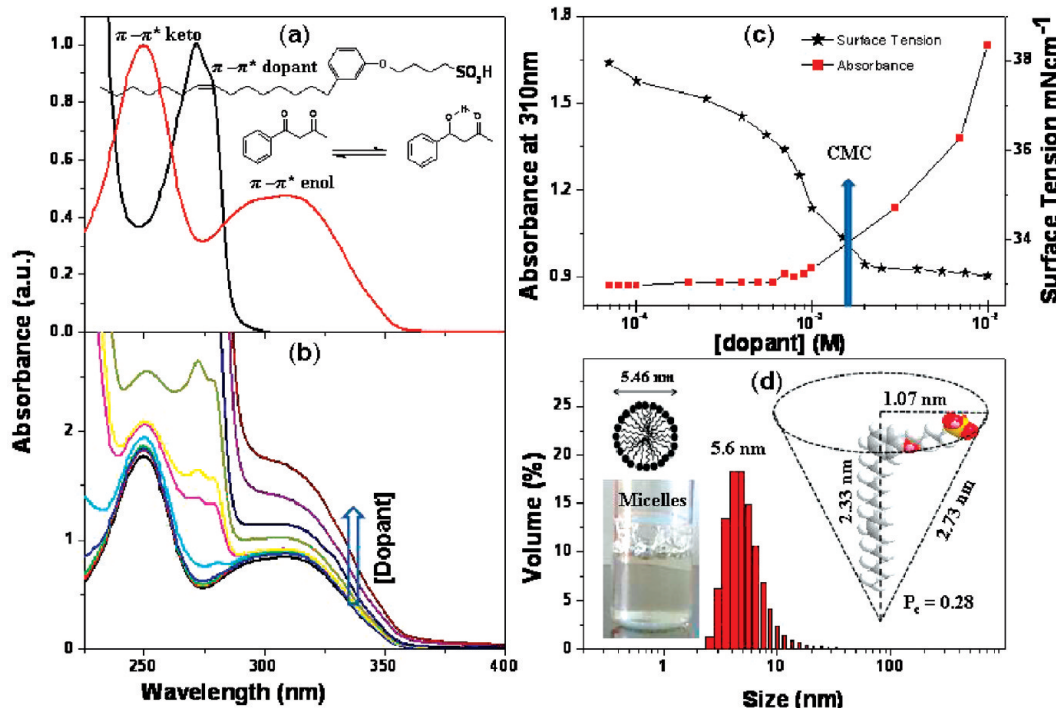


**Figure 2.** Determination of the CMC of the dopant by dye encapsulation (a,b) and surface tension (c). DLS histograms of dopant in water (d) and MM2 energy minimized structure of the dopant molecule for  $P_c$  determination.

at  $1051\text{ cm}^{-1}$  was assigned to  $\text{O}=\text{S}=\text{O}$  vibration in sulfonic acid. The sulfonic acid dopant is a white waxy solid and the thermogravimetric analysis (TGA) showed that it is thermally very stable up to  $400\text{ }^\circ\text{C}$  (see Supporting Information). The heating cycle of DSC analysis showed a broad peak around  $59\text{ }^\circ\text{C}$  corresponding to the melting of the dopant and up on cooling the crystallization peak was appeared around  $44\text{ }^\circ\text{C}$  (sees Supporting Information). It suggested that newly designed dopant is thermally stable and crystalline and easy to handle for nanomaterials research.

The new dopant has the typical amphiphilic structure with a flexible long alkyl tail and highly polar hydrophilic head bearing sulfonic acid functional groups. The dopant was highly soluble in water and formed a foamy solution (see Figure 2d). In order to understand the micellar behavior of the new amphiphilic dopant, dye encapsulation studies were carried out using absorbance spectroscopy in water.<sup>43</sup> The dye encapsulation technique is useful to determine the critical micelle concentration (CMC) of the amphiphilic dopant and also to establish the evidence for the encapsulation of organic molecules like aniline and toluene (which are similar to dye molecules) in the hydrophobic core of the dopant micelles in water. 1-Phenyl-1,3-butadione ( $\beta$ -diketone) was chosen as the dye for this purpose because it exhibits keto-enol tautomerism in water.<sup>43,44</sup> The abundances of keto and enol isomeric forms are highly dependent upon the hydrophobic (or hydrophilic) environment around the  $\beta$ -diketone moiety. The inner part of the micelles provides hydrophobic environment, and therefore  $\beta$ -diketone is expected to show large enhancement of the enol form above the CMC of the surfactant. Either the decrease in the abundance of keto-form or enhancement of enol-form directly provides information about CMC of the surfactant.  $\beta$ -Diketone has two strong absorption peaks at 254 and 310 nm for the  $\pi-\pi^*$  transition corresponding to keto and enol-form, respectively<sup>43</sup> (see Figure 2a). The amphiphilic dopant has an absorption peak at 270 nm for the  $\pi-\pi^*$  transition corresponding to phenyl ring (see Figure 2a). The comparison of the absorption spectra of

$\beta$ -diketone and dopant indicates that the enol-form (at 310 nm) of the  $\beta$ -diketone is not disturbed by the absorbance characteristics of dopant. Therefore, the changes occurred in the enol-form of the  $\beta$ -diketone during the dye-encapsulation studies can be directly utilized for determining the CMC of the amphiphilic dopant (surfactant) in water. Encapsulation experiments were carried out by keeping the amount of  $\beta$ -diketones constant ( $3.5 \times 10^{-5}\text{ M}$ ) and by varying the concentration of the dopant from  $7 \times 10^{-5}$  to  $10^{-2}\text{ M}$  in water. The concentration variation spectra are shown in Figure 2b. The intensity of the peak corresponding to enol-form (at 310 nm) was plotted against the variation of the concentration of the dopant<sup>43</sup> (Figure 2c). From the plot, the CMC of the amphiphilic surfactant dopant was determined as  $2 \times 10^{-3}\text{ M}$ . Further, to validate this CMC value we have also carried out concentration dependent surface tension measurement of the dopant solution.<sup>45</sup> The surface tension measurement (Wilhelmy plate method) was carried out in double distilled water at  $29\text{ }^\circ\text{C}$  and the plot of surface tension against surfactant concentration is depicted in Figure 2c. Below the CMC, the surface tension decreased with increase in surfactant concentration and the surface tension did not change considerably above the CMC. The CMC is taken as the concentration where the surface tension changes its trend and is found to be  $2 \times 10^{-3}\text{ M}$  at  $29\text{ }^\circ\text{C}$ . These two independent experiments confirmed that the surfactant dopant forms micelles above its CMC of  $2 \times 10^{-3}\text{ M}$ .

DLS technique is an efficient tool to measure the size of the surfactant micelles.<sup>40,46</sup> DLS data for the dopant in water for the concentration of  $1.1 \times 10^{-2}\text{ M}$  (above CMC) was shown in Figure 2d. The distribution plot showed that the amphiphilic butane sulfonic acid exists as 5.6 nm micelle in water (see Figure 2d). The micellization process in solvent was controlled by two opposing forces: (i) van der Waals attractive forces between hydrocarbon tails and (ii) electrostatic repulsion between polar hydrophilic head groups.<sup>47-49</sup> The formation of micelles by a particular surfactant can be predicted by the critical packing parameter,  $P_c = V/lal$ , where "V" is the volume occupied by

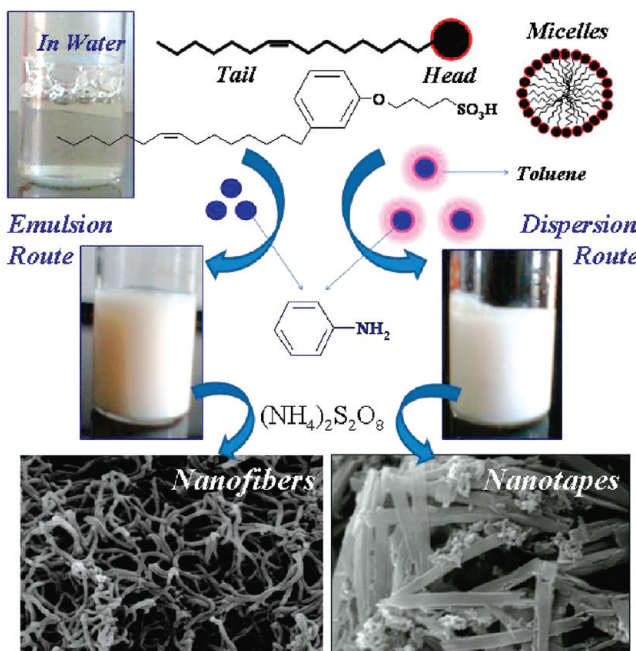


**Figure 3.** Synthesis of polyaniline nanomaterials via emulsion and dispersion routes.

hydrophobic part of the molecule, “*a*” is the headgroup area, and “*l*” is the length of the molecule.<sup>47</sup> The  $P_c$  directly correlates the expected geometry of the amphiphilic molecule self-assembly for spherical micelles ( $P_c = <0.33$ ), cylindrical micelles ( $P_c = 0.33–0.50$ ), bilayers ( $P_c = 0.50–1.0$ ), and reverse or inverted micelles ( $P_c > 1$ ).<sup>47</sup> In order to get more insight into the dopant packing factor, we have utilized energy minimized MM2 structure for calculations (see Figure 2d). The molecule has a bend shape with a headgroup radius of 1.07 nm and tail length of 2.33 nm with overall molecular length of 2.73 nm. It appears as a cone shape with a large head and a long hydrophobic tail. The  $P_c$  for the new amphiphilic dopant molecule was obtained as 0.28, which predicts the shape of the micelles as spherical one. On the basis of the energy minimized structure, the theoretical diameter of the spherical micelle (which is equivalent to the twice the end-to-end distance of the dopant) was calculated as 5.5 nm (see Figure 2d). The calculated diameter of the micelle (5.5 nm) is well matching with that of the DLS experimental value (5.6 nm). All of the independent experiments (dye encapsulation, surface tension, DLS, and  $P_c$ ) directly evidence that the newly synthesized renewable resource butane sulfonic acid amphiphilic dopant exists in the form of 5.6 nm spherical micelles in water.

Two polymerization approaches (emulsion and dispersion routes) were adopted for tuning the size and shape of the polyaniline nanostructures (see Figure 3). In emulsion route, aniline monomer (0.55 M) is added to the micellar solution of dopant in water and stirred under ultrasonic to produce a milky white emulsion<sup>37</sup> (see vial in Figure 3). In the dispersion approach, aniline is dissolved in toluene, and it was added into dopant micelles in water and stirred under ultrasonic to produce a milky white dispersion (see vial in Figure 3). In both the routes, we have taken the dopant concentration above the CMC ( $>2 \times 10^{-3}$  M, see Table 1). The composition of [aniline]/[dopant] was also varied in the feed as 10, 50, 75, and 100 (in moles) to investigate the influence of the composition and for reproducibility. The resultant emulsion or dispersion were further oxidized by ammoniumpersulfate to yield the polyaniline nanomaterials. In both the cases, the polymerization was allowed

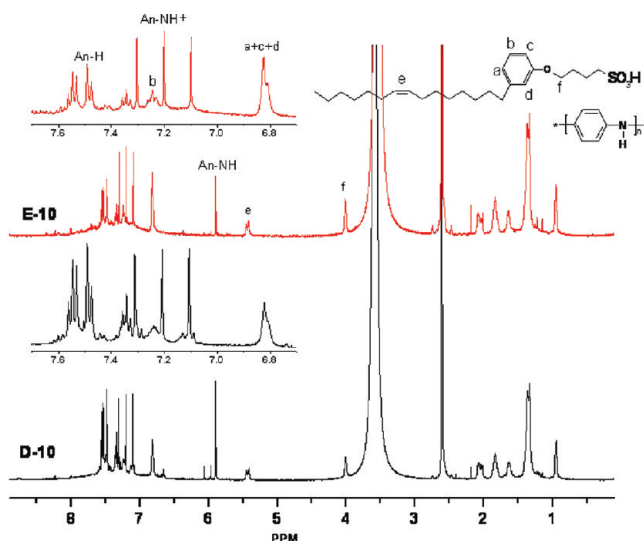


**Figure 4.**  $^1\text{H}$  NMR spectra of the polyaniline nanomaterials in  $d_6$ -DMSO.

to continue for 15 h at room temperature without any agitation, and during this period the entire reaction mixture is transformed into a dark green solid mass. It was filtered in a Buchner funnel and washed many times with distilled water followed by methanol until the filtrate became colorless. The dark green colored product was dried in a vacuum oven kept at 55 °C for 48 h and was obtained as a 60–80% yield. The samples prepared by emulsion and dispersion routes were denoted as **E-X** and **D-X**, respectively (**E** = emulsion, **D** = dispersion, and **X** = [aniline]/[dopant] ratio in the feed; see Table 1). Usually polyaniline samples (nanomaterials and also normal form) are insoluble and almost all the reports never provide their complete structural characterization by NMR. In the present case, the amphiphilic molecule makes these conducting nanostructures easily soluble in polar organic solvents like DMSO (also in NMP and DMF) for complete structural characterization by NMR.  $^1\text{H}$  NMR spectra of the polyaniline nanomaterials (**E-10** and **D-10**) were recorded in  $d_6$ -DMSO and their corresponding spectra are shown in Figure 4. The NMR spectra of the polymers showed peaks corresponding to their structures as well as dopant molecule (peaks are shown by alphabets). It confirmed the strong binding ability of sulfonic acid dopant to the polymer structure and also the doped nature of the polyaniline chains. The two peaks with characteristic splitting at 7.55 and 7.49 were assigned to protons of polyaniline chains<sup>41,50</sup> (see expanded region, Figure 4). The three equally intense peaks (1/1/1 triplet) at 7.10, 7.20, and 7.30 ppm are attributed to the protonated  $-\text{NH}$  resonance due to the  $^{14}\text{N}$  with unit spin which makes the proton attached to it split into three lines.<sup>51</sup> The peak at 5.90 ppm was assigned to unprotonated  $-\text{NH}$  present in the polymer backbone.<sup>51</sup> The spectra of **E-10** and **D-10** were almost identical indicating similarity of the polyaniline chemical structure produced via emulsion and dispersion routes. Polymers **E-50** to **E-100** and **D-50** to **D-100** were found partially soluble in DMSO and their NMR spectra are also similar to the above samples (see Supporting Information). In general, anionic surfactants behave as both surfactants for polymerization as well as counteranion dopants for the positively charged conducting polymer chains. The anionic surfactants permanently bind to the polymer chains and become an integral part of the resultant nanomaterials. The amount of sulfonic acid dopant incorporated in the polyaniline chain was determined by comparing the integral intensities of the aromatic peak intensities of the dopant

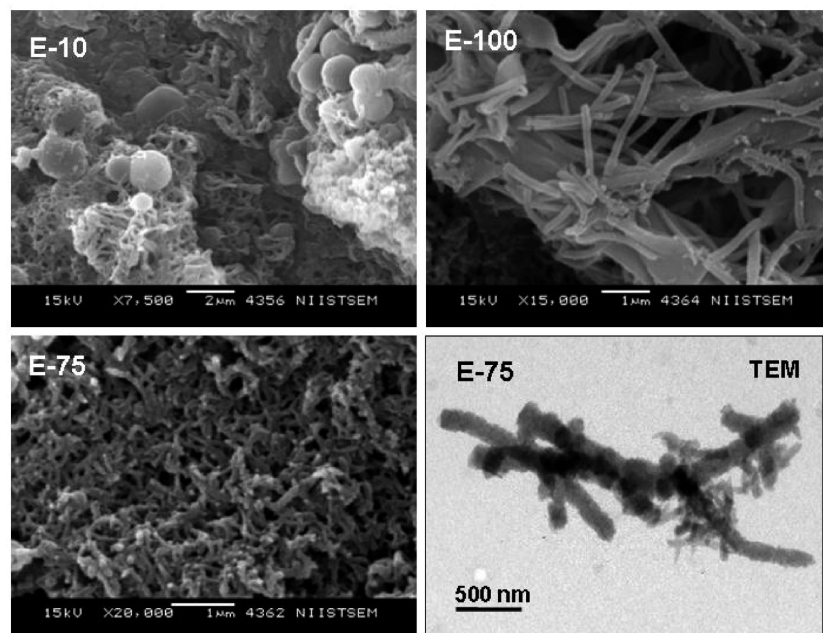


**Figure 5.** SEM and TEM images of the polyaniline nanofibers synthesized by emulsion.

(at 7.28 ppm/three protons) versus polyaniline (7.55 and 7.49 ppm together/four protons). The percentage incorporation (mol %) of dopant in the synthesized samples were reported in Table 1. The plot of incorporation of dopant in the polymer versus feed (see Supporting Information) revealed that upon decreasing the [aniline]/[dopant] ratio, the actual incorporation of dopant also decreased linearly. However, the decrease was found to be much more drastic for the dispersion route samples compared to that of those synthesized by the emulsion routes. The custom-designed new renewable resource dopant is an efficient solubilizing agent for the polyaniline chain in common organic solvents like DMSO and facilitate the complete structural characterization by NMR, which is very rarely reported in the literature.<sup>52</sup> The polyaniline samples were subjected to FT-IR analysis using KBr pellets (Supporting Information). Two peaks that appeared at 1582 and 1501  $\text{cm}^{-1}$  were assigned to the quinoid and benzenoid ring C=C stretching ring deformations, respectively.<sup>53</sup> The peaks at 1315 and 832  $\text{cm}^{-1}$  were assigned to C–N stretching and C–H out-of-plane vibrations of 1,4-disubstituted benzene ring, respectively, and the peak at 2932  $\text{cm}^{-1}$  corresponds to –C–H vibrations.<sup>54</sup> Four peaks present in the samples at 1307, 1026, 830, and 630  $\text{cm}^{-1}$  were assigned to O=S=O (sym), NH<sup>+</sup>..... SO<sub>3</sub><sup>-</sup> interactions between the polymers chain and the dopant, S–O (unsym) and C–S stretching vibrations, respectively.<sup>55</sup> The inherent viscosity of the polymer samples **E-10** to **E-100** and **D-10** to **D-100** (in PANI-EB form) was determined for 0.5 wt % solutions in NMP at 30 °C. The inherent viscosities of the polymers were obtained in the range of  $\eta_{inh} = 0.23\text{--}0.28 \text{ dL/g}$  (see Supporting Information). The viscosities of the samples indicate the formation of good molecular weight samples and the values are comparable to that of earlier reports for polyaniline materials.<sup>56–58</sup> The thermal stability of the polymer samples were analyzed by TGA, and the plots indicated that the polyaniline nanomaterials were very stable up to 300 °C and useful for high temperature applications (see Supporting Information).

The morphologies of the nanostructures were recorded using JEOL JSM- 5600 LV scanning electron microscope. The SEM images of the emulsion route nanomaterials **E-10** to **E-100** are given in Figure 5. The sample **E-10** has both dendritic nanofibers

and micrometer size spheres. **E-75** contains nanofibers of diameter  $\sim 80 \text{ nm}$  with an average length up to  $2 \mu\text{m}$ . **E-100** also contains only nanofibers with average 100 nm diameter and length of 3–5  $\mu\text{m}$ . TEM image of **E-75** (see Figure 5) confirmed the morphology as nanofibers of diameter 100 nm with length up to  $2.5 \mu\text{m}$  (similar to its SEM image). The SEM-images of dispersion route samples **D-10** to **D-100** are given in Figure 6. It is very interesting to note that the samples synthesized through dispersion route were exclusively planar nanotapes and completely different from that those produced by emulsion route. **D-10** contains very long tape but the morphology is not very uniform. In **D-50** and **D-75**, the morphology of the nanotape was very uniform and the width and thickness were obtained as 200 and 30 nm, respectively (see expanded SEM-image). The average lengths of the nanotapes were obtained as  $1.8 \pm 0.25 \mu\text{m}$ . The expanded image of nanotapes (**D-50**) shows a sawtooth kind of edge with rough surface that is an indicative of template-mediated growth of nanotapes. Sample **D-100** contains stacked nanotapes with small amount of particulate aggregates. The TEM image (**D-75**, Figure 6) clearly demonstrated the flat and tapelike nature of the nanostructures. From the microscopic analysis of the nanomaterials, it is very clear that the types of polymerization play a major role in the determination of the morphologies. The emulsion and dispersion routes exclusively produce nanofibers and nanotapes, respectively. The shape and size of the nanomaterials were not altered and are reproducible for wider composition range ([aniline]/[dopant] = 50 to 100) that further confirmed that morphology evolution was primarily driven by the polymerization processes.

The morphology studies suggest that the dopant molecules behave differently in emulsion and dispersion routes and produce exclusively only one particular type nanomaterials. Therefore, it is very important to understand the mechanistic aspects of the amphiphilic dopant in the polymerization process. DLS technique is an efficient tool to study the micellar structures in solution.<sup>59,60</sup> DLS measurements were carried out for both emulsion (dopant + aniline) and dispersion (dopant + aniline + toluene) templates in water (see Figure 7). The addition of aniline to dopant micelles in water produces milky white thick

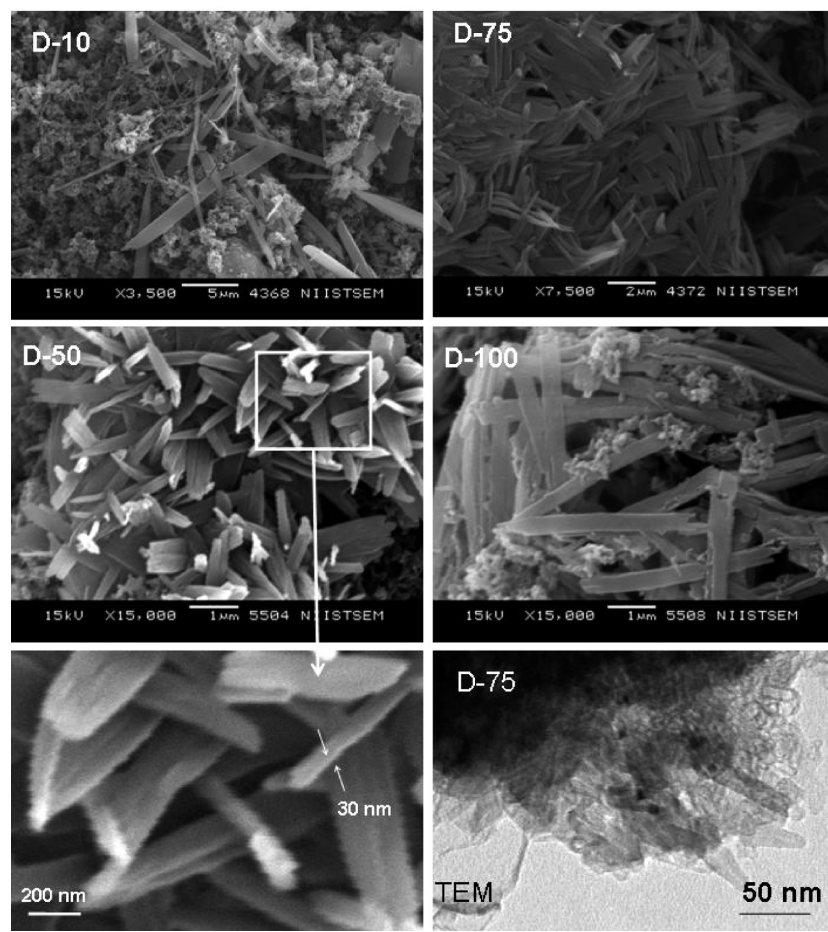


**Figure 6.** SEM and TEM images of the polyaniline nanotapes synthesized by dispersion.

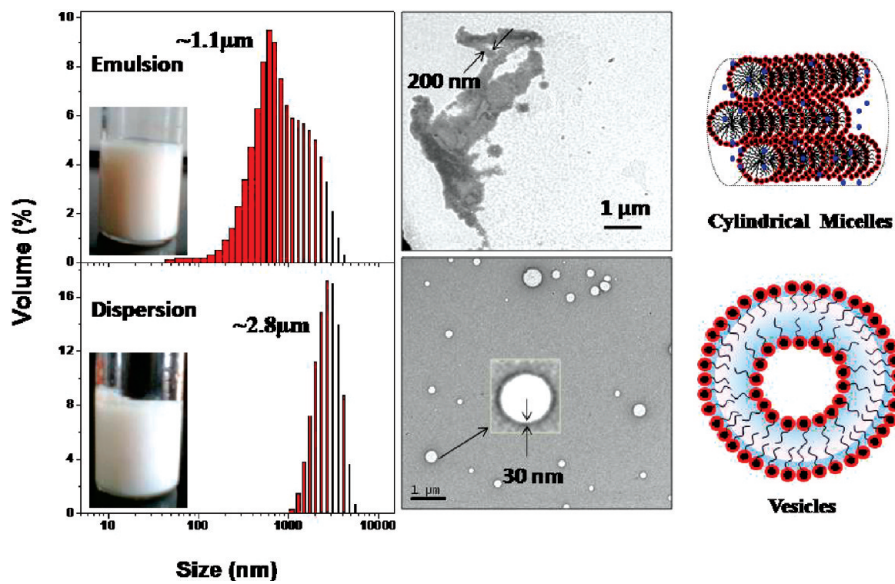


**Figure 7.** Templates characterization by DLS and HRTEM and corresponding schematic representation of cylindrical and vesicular templates.

emulsion and DLS data of the resultant emulsion showed the presence of aggregates of  $1.1\text{ }\mu\text{m}$ . Similarly the addition of aniline in toluene into dopant micelles in water and subsequent ultrasonication resulted in the formation of a white stable dispersion. The DLS of this dispersion showed the presence of aggregates of sizes around  $2.8\text{ }\mu\text{m}$ . The dispersion templates are found to be more narrowly distributed compared to that of emulsion templates. DLS experiments show evidence that the amphiphilic dopant molecule has behaved as a typical surfactant-

cum-dopant and formed stable micellar aggregates with aniline or aniline in toluene under the polymerization conditions. The DLS data provide the existence of the micrometer-sized aggregates in emulsion and dispersion routes, but it cannot predict the shape and type of the aggregates. The polymerization mixtures were very stable and drop cast on TEM grid for visualizing these aggregates microscopically to map out the shape of the templates.<sup>59,61</sup> HRTEM images of the polymerization templates are shown in Figure 7. The emulsion template

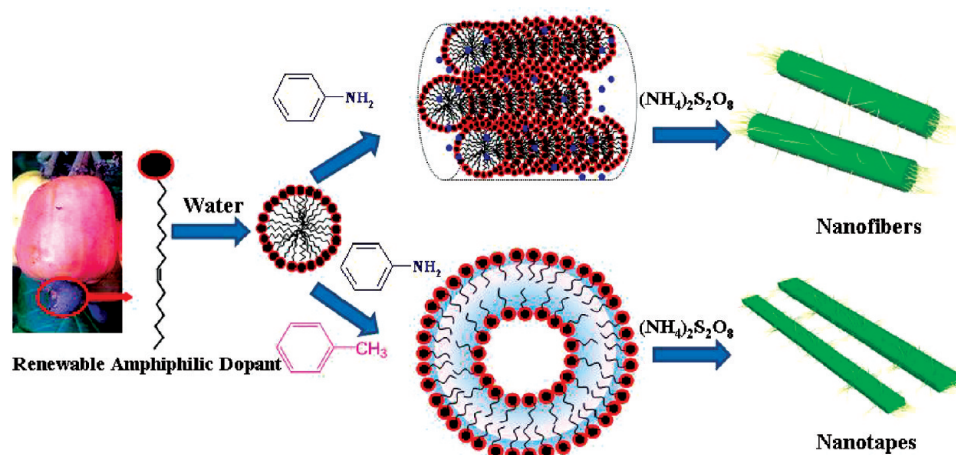


**Figure 8.** Plausible mechanism of polyaniline nanostructures via selective templating in emulsion (top) and dispersion (bottom) routes.

(E-50) showed cylindrical micellar aggregates of  $\sim 150$  nm diameter with length up to  $1\text{--}3 \mu\text{m}$ . It suggests that the addition of aniline induces self-organization in the amphiphilic dopant micelles and the resultant cylindrical micelles template for the formation of polyaniline nanofibers. The transition from spherical to cylindrical micelles upon adding aniline was observed by us in earlier studies and by other researchers also.<sup>40,61,62</sup> The formation of cylindrical aggregated micelles can be explained by the acid–base interaction between the sulfoicacid head part of the amphiphilic dopant with basic aniline. The size of the micelle aggregates (see Figure 7) and the synthesized nanofibers' dimensions (SEM and TEM images) are matching well within experimental variation. This directly gives evidence for the cylindrical micellar aggregates template-mediated process in the emulsion polymerization route. TEM image of dispersion route polymerization mixture (D-50) showed completely different types of template morphology compared to its emulsion route. The dispersion template contains exclusively spherical vesicles and the sizes of the vesicles appeared as  $\sim 450 \pm 200$  nm in diameter with wall thickness of  $20 \pm 10$  nm. The size of aggregates obtained by DLS showed a discrepancy with TEM observation; we believe that in solution there are high degrees of aggregation among the vesicles that overestimate the values in DLS. Since the TEM sample preparation was carried out at a much lower concentration, the isolate vesicles could be observed. It has been well known in the literature that typical amphiphilic molecules can exist in the dynamic equilibrium between vesicle and cylindrical micellar aggregates depending upon the concentration or external induction by organic molecules.<sup>63–65</sup> Two types of competition interactions are possible when aniline + toluene are added into the dopant micelles in water. (i) The basic aniline molecule can interact with sulfonic acid part of the micelles in water to produce cylindrical aggregates via acid–base interaction (as similar to emulsion route) and (ii) the toluene molecules tend to stack in the aromatic part of the micelles, which induced the transformation of the templates into vesicular aggregates. Recently Raghavan and co-workers had reported a similar transformation of wormlike cylindrical micelles into unilamellar vesicles upon adding aromatic molecules like salicylicacid via selective aromatic ring interactions.<sup>63</sup> Hence, the addition of excess organic phase (toluene) is expected to increase the packing parameter ( $P_c$ ) and the spherical dopant micelles transformed into a shape with very low-curvature aggregate-like vesicles. These resultant vesicular aggregates behave as templates for formation of nanotapes in dispersion route.

A plausible mechanism of self-organized amphiphilic dopant-driven polyaniline nanostructures formation is proposed as given in Figure 8. The amphiphilic sulfonic acid dopant exists in the form of 5.6 nm micelles in water. The complexation of spherical micelles with aniline produce large micrometer size ( $1.1 \mu\text{m}$  range) cylindrical micellar aggregates that behave as templates in emulsion route for the formation of nanofibers. In the dispersion route, upon adding aniline dissolved in toluene into dopant micelles in water produced vesicular aggregates that template for nanotapes. One would immediately ask the question of how do nanotapes evolve from vesicular hollow structures? Recent reports based on the self-organization of sugar derivatives of cardanol documented the formation of vesicles and subsequent transformation of vesicles into long twisted tapes.<sup>66,67</sup> Prolonged storage of the twisted nanotapes subsequently undergoes transformation into nanotubes. Though the mechanism of the opening of the vesicles to nanotapes is still under debate, the transformation was confirmed by many examples.<sup>66,68</sup> Therefore, we believe that the vesicular template may open during subsequent oxidative polymerization process to form polyaniline nanotapes. The ripping of vesicles can be further confirmed from the sawtooth type edges in the surface of the nanotapes (see Figure 6). In order to provide evidence for the ripping of vesicular templates, we have compared the dimensions of the vesicles and the resultant nanomaterials. The average diameter ( $2r$ , where  $r$  is the radius) of a vesicle is  $0.6 \mu\text{m}$  which give the circumference of the vesicle ( $2\pi r$ ) as  $1.9 \mu\text{m}$ . The average lengths of the nanotapes synthesized from the vesicular templates was obtained as  $1.7 \pm 0.4 \mu\text{m}$  (from SEM images). The circumference of vesicular template is very well matching with that of the average length of the nanotapes. Second, the thickness of the nanotapes and vesicular templates wall thickness were found almost identical ( $\sim 30$  nm). It is directly evident that the nanotapes formed from the vesicular templates. During the chemical oxidation of the vesicular templates by APS, the vesicles are ripped in the surface to form the nanotapes. The above results suggest that the newly designed renewable resource amphiphilic dopant is an efficient structure directing agent for polyaniline nanofiber or nanotapes via selective self-assembled template processes. The newly designed amphiphilic surfactant bears an aliphatic sulfonic acid polar group with a long tail consisting of aromatic benzene ring and aliphatic pentadecylene chain. Therefore, the nature and behavior of the new amphiphilic is expected to be different from the typical sulfonic acid surfactants like aromatic sulfonic acids (like DBSA) or aliphatic sodium dodecyl sulfonic acid (SDS).

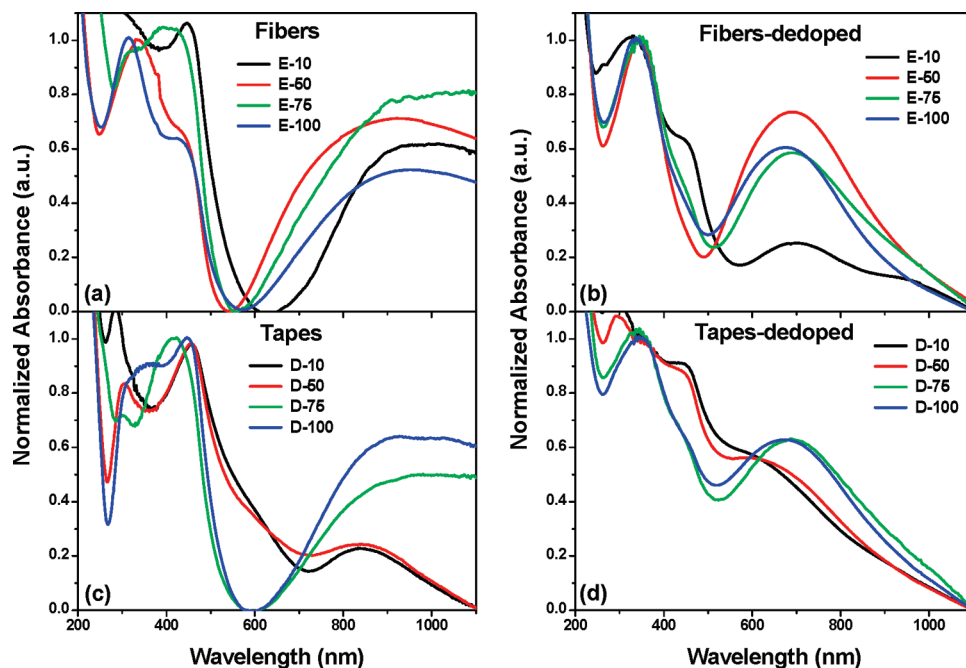


**Figure 9.** UV-vis absorption spectra of polyaniline nanomaterials in doped and dedoped form in water at 30 °C.

Amphiphilic azobenzene sulfonic acid reported by us in earlier report<sup>36–41</sup> was found not soluble in organic medium, which restricts its usage for dispersion route. Therefore, the appropriate sizes of the polar head and hydrophobic tail are crucial factors in the successful templating behavior of amphiphilic dopants. We believe that the unique structural features associated with new dopant design enhances its solubility in variety of organic solvents as well as in water which facilitate its different types of template formation in emulsion and dispersion routes.

The nanostructures are highly water suspendable and the green-colored colloidal solutions are stable for 2–3 days at ambient conditions. In order to study the conformational as well as oxidation state of the polymer chains present in nanomaterials, we have recorded the UV-vis spectra of the pristine as well as dedoped form of nanostructures in water and shown in Figure 9. It is clear from the plots of nanofiber samples (see Figure 9) that it contains all the characteristic peaks of doped polyaniline, the peaks at 360, 450, and 800 nm, which were assigned as the transitions from  $\pi-\pi^*$  band, polaron band to  $\pi^*$  band, and  $\pi$  band to polaron band, respectively.<sup>69,70</sup> It is also seen that in all four cases there is a tailing nature in the NIR region of the spectra indicating more expanded nature of polyaniline chain.<sup>69</sup> The spectra of **D-75** and **D-100** were very similar to that of nanofiber samples and exhibited the characteristic peaks of highly doped expanded emeraldine salt form of polyaniline, however, the intensity of polaron peak for **D-10** and **D-50** were relatively low. The spectra of dedoped form of all the nanofiber samples (**E-10** to **E-100**, see Figure 9) showed peaks at 360 and 650 nm as similar to conventional emeraldine base (EB) form.<sup>71</sup> The spectra of dedoped nanotapes **D-75** and **D-100** also showed similar characteristics of emeraldine base with absorption maxima at 650 nm. In the case of **D-10** and **D-50**, the absorption maxima was blue shifted by 50 nm, which indicates the presence of pernigraniline form along with EB form in nanotapes. The reason for the pernigraniline structure in dispersion route may be correlated to over oxidation of polyaniline emeraldine chains at the organic/aqueous interface at the initial stages of polymerization.<sup>60</sup> The bulk conductivity of the polyaniline nanostructures was determined by four probe

conductivity measurements for compressed pellets at room temperature and the values are reported in Table 1. The conductivities of the samples were found in the range of 0.03–0.44 S cm<sup>-1</sup> which is in accordance with sulfonic acid doped polyaniline samples.<sup>20,36</sup> Additionally the four probe conductivity of *m*-cresol cast films of nanomaterials also was measured and it showed a one order higher value in the range of 0.2–8.8 S cm<sup>-1</sup> than corresponding pellets (see Table 1). It is well known in polyaniline literature that *m*-cresol has a secondary doping effect and also orders the polyaniline chains for improved electrical properties of polyaniline.<sup>70</sup>

The new dopant has an amphiphilic structure so it is expected to penetrate into polyaniline chains and may result in the formation of layered structures.<sup>72</sup> These types of layered dopant–polymer supramolecular structures are expected to reflect on the low-angle region of the wide angle X-ray diffraction (WXRD) patterns<sup>72–74</sup> (low  $2\theta$  values, higher *d*-spacing). In order to investigate the solid-state properties of polyaniline nanostructures, the nanomaterials were finely powdered and subjected for WXRD. The WXRD patterns of polyaniline nanostructures synthesized by emulsion and dispersion method are shown in Figure 10. Both nanofibers and nanotapes showed a broad peak at  $2\theta = \sim 25^\circ$  with respect to aromatic chain interactions. Emulsion route synthesized nanofibers showed a sharp lower angle peak at  $2\theta = 3.3^\circ$  (*d*-spacing of 26 Å) corresponding to highly solid state ordered structure. Dispersion route nanotapes samples showed two peaks at the low angle region at  $2\theta = 3.3^\circ$  peak and  $2\theta = 6.4^\circ$  (*d* = 13.7 Å). The peak at  $2\theta = 6.4^\circ$  was observed by us and others for polyaniline structures in which sulfonic acids were employed as dopants.<sup>36–41</sup> Therefore, the peak at *d* = 13.7 Å is the resultant of sulfonic acid interactions with polyaniline chains which induced short-range solid state ordering. However, this is for the first time both peaks at  $2\theta = 3.3^\circ$  (corresponding to long-range ordering) and  $6.4^\circ$  (short-range ordering) were observed in the same polyaniline nanomaterials doped by amphiphilic dopants. In both nanofibers and nanotapes, the  $3.3^\circ$  peak has *d*-spacing value of 26 Å, which is comparable to the molecular length 27 Å of the amphiphilic dopant molecule. This indicates

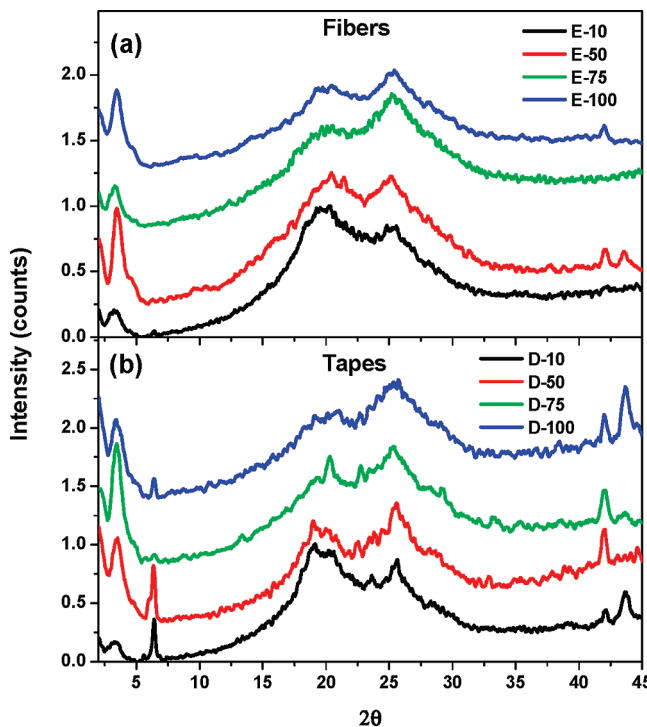


**Figure 10.** WXRD pattern of polyaniline nanomaterials at 30 °C.

that the peaks at 26 and 13.7 Å represent the first and second order reflection in the lamellae of the nanostructures. It revealed that the polyaniline nanostructures may exist as lamellar type polyaniline–sulfonate supramolecular complex with stacks of polymer chains are separated by dopant anions. These layered lamellae may be formed due to the interdigitations and crystallization of side chains of the doped polyaniines. Further studies are required to understand and confirm the supramolecular structures of the polyaniline nanomaterials.

## Conclusions

We have developed a novel amphiphilic sulfonic acid dopant from cardanol which is successfully utilized as structure directing agent for polyaniline nanomaterials—nanofibers and nanotapes by emulsion and dispersion routes, respectively. This dopant-based approach has the following merits: (i) a new dopant was developed from renewable resource waste cardanol by ring-opening of sultone under basic conditions, which opens up new possibilities for designing novel amphiphilic molecules; (ii) the dopant forms micelle in water and its CMC was determined by multiple techniques such as dye encapsulation, surface tension, and DLS methods; (iii) the micelles formed by the dopant is utilized to grow polyaniline nanostructures under emulsion and dispersion routes; (iv) in emulsion route the cylindrical micellar soft template formed between dopant and aniline leads to the formation of nanofibers whereas in the dispersion route the vesicular template of aniline + toluene produced nanotapes; (v) the polyaniline nanostructures are soluble in high polar solvents like DMSO that enabled us the complete structural characterization and composition determination by NMR; (vi) DLS and HR-TEM techniques were successfully utilized to understand the mechanistic aspects of nanostructure formation; (vii) the absorption spectra of nanomaterials showed that all are in highly doped expanded chain nature; and (viii) the WXRD studies confirmed the layered lamellar type packing of polymer chains in nanomaterials. The polyaniline nanomaterials are highly soluble and therefore they

may suitable for various applications in bio and chemical sensors and optical devices. To summarize, we have shown for the first time that a novel renewable resource amphiphilic dopant is a good candidate for the synthesis of high quality nanofibers and nanotapes by carefully choosing the amphiphilic dopant templates under emulsion and dispersion polymerizations in a single system.

**Acknowledgment.** We thank Department of Science and Technology, New Delhi, India under Scheme: NSTI Programme SR/S5/NM-06/2007 and SR/NM/NS-42/2009 for financial support. The authors thank Mr. M. R. Chandran, Dr. V. S. Prasad, Mr. P. Gurusamy, Mr. Adarsh, and Mr. P. Mukundan of NIIST-Trivandrum for SEM, TEM, WXRD, NMR, and surface tension measurements. We also thank Dr. C. P. Sharma and Mr. Willi Paul, SCTIMST, Trivandrum for dynamic light scattering analysis. P.A. thanks UGC-New Delhi, India for senior research fellowship.

**Supporting Information Available:** Mass, DSC, TGA, and FTIR plots of dopant molecule, NMR, viscosity, TGA, FTIR, and cyclic voltammogram details of nanomaterials, and theoretical details on DLS studies are available. This material is available free of charge via the Internet at <http://pubs.acs.org>.

## References and Notes

- (1) Li, D.; Huang, J.; Kaner, R. B. *Acc. Chem. Res.* **2009**, *42*, 135–145.
- (2) Wan, M. X. *Adv. Mater.* **2008**, *20*, 2926–2932.
- (3) Zhang, D. H.; Wang, Y. Y. *Mater. Sci. Eng., B* **2006**, *134*, 9–19.
- (4) Zhang, X.; Goux, W. J.; Manohar, S. K. *J. Am. Chem. Soc.* **2004**, *126*, 4502–4503.
- (5) Wang, C. W.; Wang, Z.; Li, M. K.; Li, H. L. *Chem. Phys. Lett.* **2001**, *341*, 431–434.
- (6) Hatchett, D. W.; Josowicz, M. *Chem. Rev.* **2008**, *108*, 746–769.
- (7) Haung, J.; Virji, S.; Weiller, B. H.; Kaner, R. B. *Chem.—Eur. J.* **2004**, *10*, 1314.
- (8) Anilkumar, P.; Jayakannan, M. *Langmuir* **2008**, *24*, 9754–9762.
- (9) Ma, Y.; Ali, S. R.; Dodo, A. S.; He, H. *J. Phys. Chem. B* **2006**, *110*, 16359–16365.
- (10) Baker, C. O.; Shedd, B.; Innis, P. C.; Whitten, P. G.; Spinks, G. M.; Wallace, G. G.; Kaner, R. B. *Adv. Mater.* **2008**, *20*, 155.
- (11) Martin, C. R. *Acc. Chem. Res.* **1995**, *28*, 61.
- (12) Meng, L.; Lu, Y.; Wang, X.; Zhang, J.; Duan, Y.; Li, C. *Macromolecules* **2007**, *40*, 2981–2983.
- (13) Huang, L.; Wang, Z.; Wang, H.; Cheng, X.; Mitra, A.; Yan, Y. J. *Mater. Chem.* **2002**, *12*, 388–391.
- (14) Wei, Z.; Zhang, Z.; Wan, M. X. *Langmuir* **2002**, *18*, 917–921.
- (15) Zhang, Z.; Wei, Z.; Wan, M. X. *Macromolecules* **2002**, *35*, 5937–5942.
- (16) Chattopadhyay, D.; Mandal, B. M. *Langmuir* **1996**, *12*, 1585–1588.
- (17) Armes, S. P.; Aldissi, M.; Hawley, M.; Berry, J. G.; Gottesfeld, S. *Langmuir* **1991**, *7*, 1447.
- (18) Haung, J.; Virji, S.; Weiller, B. H.; Kaner, R. B. *J. Am. Chem. Soc.* **2003**, *125*, 314.
- (19) Chiou, N. R.; Epstein, A. J. *Adv. Mater.* **2005**, *17*, 1679–1683.
- (20) Haung, K.; Wan, M. X. *Chem. Mater.* **2002**, *14*, 3486–3492.
- (21) Yan, Y.; Yu, Z.; Huang, Y. W.; Yuan, W. X.; Wei, Z. X. *Adv. Mater.* **2007**, *19*, 3353.
- (22) Haung, J.; Kaner, R. B. *J. Am. Chem. Soc.* **2004**, *126*, 851–855.
- (23) Zhang, L.; Wan, M. X. *J. Phys. Chem. B* **2003**, *107*, 6748–6753.
- (24) Zhou, C.; Han, J.; Guo, R. *J. Phys. Chem. B* **2008**, *112*, 5014–5019.
- (25) Stejskal, J.; Kratochvil, P.; Gospodinova, N.; Terlemezyan, L.; Mokreva, P. *Polym. Commun.* **1992**, *33*, 4857.
- (26) Palaniappan, S.; John, A. *Prog. Polym. Sci.* **2008**, *33*, 732–758.
- (27) Lee, S. H.; Lee, D. H.; Lee, K.; Lee, C. W. *Adv. Funct. Mater.* **2005**, *15*, 1495–1500.
- (28) Jing, X.; Wang, Y.; Wu, D.; She, L.; Guo, Y. *J. Poly. Sci. Part A: Polym. Chem.* **2006**, *44*, 1014–1019.
- (29) Li, D.; Kaner, R. B. *J. Am. Chem. Soc.* **2006**, *128*, 968–975.
- (30) Haung, J.; Kaner, R. B. *Angew. Chem.* **2004**, *116*, 5941–5945.
- (31) Zhang, L.; Peng, H.; Kilmarin, P. A.; Soeller, C.; Sejdic, J. T. *Macromolecules* **2008**, *41*, 7671–7678.

- (32) Trchova, M.; Sedenkova, I.; Konyushenko, E. N.; Stejskal, J.; Holler, P.; Marjanovic, G. C. *J. Phys. Chem. B* **2006**, *110*, 9461–9468.
- (33) Wang, Y.; Jing, X. *J. Phys. Chem. B* **2008**, *112*, 1157–1162.
- (34) Kinlen, P. J.; Liu, J.; Ding, Y.; Graham, C. R.; Remsen, E. E. *Macromolecules* **1998**, *31*, 1735–1744.
- (35) Kuramoto, N.; Tomita, A. *Polymer* **1997**, *38*, 3055–3058.
- (36) Anilkumar, P.; Jayakannan, M. *Langmuir* **2006**, *22*, 5952–5957.
- (37) Anilkumar, P.; Jayakannan, M. *J. Phys. Chem. C* **2007**, *111*, 3591–3600.
- (38) Anilkumar, P.; Jayakannan, M. *Macromolecules* **2007**, *40*, 7311–7319.
- (39) Jinish Antony, M.; Jayakannan, M. *J. Phys. Chem. B* **2007**, *111*, 12772–12780.
- (40) (a) Anilkumar, P.; Jayakannan, M. *Macromolecules* **2008**, *41*, 7706–7711. (b) Anilkumar, P.; Jayakannan, M. *J. Appl. Polym. Sci.*, in press.
- (41) Jinish Antony, M.; Jayakannan, M. *J. Polym. Sci., Part B: Polym. Phys.* **2009**, *47*, 830–846.
- (42) Santos, M. L.; Magabhaes, G. C. *J. Braz. Chem. Soc.* **1999**, *10*, 13–20.
- (43) Dominguez, A.; Fernandez, A.; Gonzalez, N.; Iglesias, E.; Montenegro, L. *J. Chem. Educ.* **1997**, *74*, 1227–1231.
- (44) Iglesias, E. *J. Phys. Chem.* **1996**, *100*, 12592–12599.
- (45) Franke, D.; Egger, C. C.; Smarsly, B.; Faul, C. F. J.; Tiddy, G. J. T. *Langmuir* **2005**, *21*, 2704–271.
- (46) Vethamuthu, M. S.; Feitosa, E.; Brown, W. *Langmuir* **1998**, *14*, 1590–1596.
- (47) Hamley, I. W. *Introduction to Soft Matter*, 2nd ed.; Wiley: New York, 2007; pp 200–204.
- (48) Tanford, C. *Proc. Nat. Acad. Sci. U.S.A.* **1974**, *71*, 1811–1815.
- (49) Israelachvili, J. N.; Mitchell, D. J.; Ninham, B. W. *J. Chem. Soc. Faraday Trans.* **1976**, *72*, 1525.
- (50) Zhou, C.; Han, J.; Song, G.; Guo, R. *J. Polym. Sci., Part A: Polym. Chem.* **2008**, *46*, 3563.
- (51) Mu, S.; Yang, Y. *J. Phys. Chem. B* **2008**, *112*, 11558.
- (52) Goto, H.; Akagi, K. *Macromolecules* **2002**, *35*, 2545–2551.
- (53) Zheng, W.; Angelopoulos, M.; Epstein, A. J.; MacDiarmid, A. G. *Macromolecules* **1997**, *30*, 7634–763.
- (54) Li, X. G.; Wang, H. Y.; Huang, M. R. *Macromolecules* **2007**, *40*, 1489–1496.
- (55) Jayakannan, M.; Anilkumar, P.; Sanju, A. *Eur. Polym. J.* **2006**, *42*, 2623–2631.
- (56) Kim, B. J.; Oh, S. G.; Han, M. G.; Im, S. S. *Synth. Met.* **2001**, *122*, 297–304.
- (57) Erdem, E.; Karakısla, M.; Sacak, M. *Eur. Polym. J.* **2004**, *40*, 785–791.
- (58) Jayakannan, M.; Annu, S.; Ramalekshmi, S. *J. Polym. Sci., Part B: Polym. Phys.* **2005**, *43*, 1321.
- (59) Buchholz, T.; Sunb, Y.; Loo, Y. L. *J. Mater. Chem.* **2008**, *18*, 5835–5842.
- (60) Zhang, X.; Kolla, H. S.; Wang, X.; Raja, K.; Manohar, S. K. *Adv. Funct. Mater.* **2006**, *16*, 1145–1152.
- (61) Zhang, L.; Wan, M. X. *Adv. Funct. Mater.* **2003**, *13*, 815–820.
- (62) Hassan, P. A.; Sawant, S. N.; Bagkar, N. C.; Yakhmi, J. V. *Langmuir* **2004**, *20*, 4874–4880.
- (63) Davies, T. S.; Ketner, A. M.; Raghavan, S. R. *J. Am. Chem. Soc.* **2006**, *128*, 6669–6675, 9 6669.
- (64) Hassan, P. A.; Valaulikar, B. S.; Manohar, C.; Kern, F.; Bourdieu, L.; Candau, S. *J. Langmuir* **1996**, *12*, 4350–4357.
- (65) Yin, H.; Lei, S.; Zhu, S.; Huang, J.; Ye, J. *Chem.—Eur. J.* **2006**, *12*, 2825–2835.
- (66) John, G.; Jung, J. H.; Masuda, M.; Shimizu, T. *Langmuir* **2004**, *20*, 2060–2065.
- (67) John, G.; Jung, J. H.; Minamikawa, H.; Yoshida, K.; Shimizu, T. *Chem.—Eur. J.* **2002**, *8*, 5494.
- (68) Nakashima, N.; Asakuma, S.; Kunitake, T. *J. Am. Chem. Soc.* **1985**, *107*, 509–510.
- (69) Xis, Y.; Wiesinger, J. M.; MacDiarmid, A. G. *Chem. Mater.* **1995**, *7*, 443–445.
- (70) MacDiarmid, A. G.; Epstein, A. J. *Synth. Met.* **1995**, *69*, 85–92.
- (71) Kang, E. T.; Neoh, K. G.; Tan, K. L. *Prog. Polym. Sci.* **1998**, *23*, 211–324.
- (72) Dufour, B.; Rannou, P.; Fedorko, P.; Djurado, D.; Travers, J. P.; Pron, A. *Chem. Mater.* **2001**, *13*, 4032–4040.
- (73) Jana, T.; Nandi, A. K. *Langmuir* **2000**, *16*, 3141.
- (74) Laska, J.; Djurado, D.; Lunzy, W. *Eur. Polym. J.* **2002**, *38*, 947–951.

JP9043418